Transient Exposure of Hydrophobic Surface in the Photoactive Yellow Protein Monitored with Nile Red

Johnny Hendriks,* Thomas Gensch,† Lene Hviid,‡ Michael A. van der Horst,* Klaas J. Hellingwerf,* and Jasper J. van Thor§

*Laboratory for Microbiology, Swammerdam Institute for Life Sciences (SILS), BioCentrum, University of Amsterdam, Nieuwe Achtergracht 166, 1018 WV Amsterdam, The Netherlands; †Institute of Biological Informationprocessing 1, Research Centre Jülich, D-52425 Jülich, Germany; ‡Institute of Molecular Chemistry, Department of Chemistry, University of Amsterdam, Nieuwe Achtergracht 129, 1018 WS Amsterdam, The Netherlands; and §University of Oxford, Laboratory for Molecular Biophysics, Rex Richards Building, Oxford, OX1 3QU, United Kingdom

ABSTRACT In this study we have investigated binding of the fluorescent hydrophobicity probe Nile Red to the photoactive yellow protein (PYP), to characterize the exposure and accessibility of hydrophobic surface upon formation of the signaling state of this photoreceptor protein. Binding of Nile Red, reflected by a large blue shift and increase in fluorescence quantum yield of the Nile Red emission, is observed exclusively when PYP resides in its signaling state. N-terminal truncation of the protein allows assignment of the region surrounding the chromophore as the site where Nile Red binds to PYP. We also observed a pH dependence of the affinity of Nile Red for pB, which we propose is caused by pH dependent differences of the structure of the signaling state. From a comparative analysis of the kinetics of Nile Red binding and transient absorption changes in the visible region we can conclude that protonation of the chromophore precedes the exposure of a hydrophobic surface near the chromophore binding site, upon formation of the signaling state. Furthermore, the data presented here favor the view that the signaling state is structurally heterogeneous.

INTRODUCTION

The photoactive yellow protein (PYP) from *Halorhodospira halophila* (formerly *Ectothiorhodospira halophila*) is a 14-kDa cytoplasmic photoreceptor protein that has been extensively studied in recent years. The chromophore, responsible for light-activation of PYP, is *p*-coumaric acid linked to Cys-69 via a thiol-ester bond. It undergoes a *trans* to *cis* isomerization during the initial stage of the photocycle of PYP. The molecular properties that characterize the main transformation events during the photocycle of PYP have been addressed by protein-folding thermodynamics (Hoff et al., 1999; Van Brederode et al., 1996), (time-resolved) Fourier transform infrared (FTIR) spectroscopy (Hoff et al., 1999; Xie et al., 1996, 2001; Brudler et al., 2001), time-resolved photoacoustic and photothermal spectroscopy (van Brederode et al., 1995; Takeshita et al., 2000), time-resolved crystallography (Genick et al., 1997a; Perman et al., 1998), crystallography of a cryo-trapped photocycle intermediate (Genick et al., 1998), nuclear magnetic resonance (NMR) spectroscopy (Rubinstenn et al., 1998; Craven et al., 2000), proton-transfer measurements (Hendriks et al., 1999a), hydrogen-deuterium exchange studies (Hoff et al., 1999; Craven et al., 2000), and circular dichroism spectroscopy combined with 8-anilinonaphthalene-1-sulfonate (ANS) probe binding experiments (Lee et al., 2001). Briefly, the ground state (pG), when excited in its absorption maximum at 446 nm, is transformed into a red-shifted intermediate (pR, absorbing maximally at 465 nm) in the picosecond to nanosecond timescale with a photo-isomerized chromophore configuration (Meyer et al., 1987; Hoff et al., 1994). On a microsecond to millisecond timescale, the pR state is transformed into a blue-shifted intermediate (pB, absorbing maximally at 355 nm). During the pR to pB transition the chromophore becomes protonated, which causes the hypsochromic band shift. The ground state is recovered from pB on a millisecond to second timescale, depending on pH, with concomitant deprotonation and *cis* to *trans* reisomerization of the chromophore.

The longest-lived photocycle-intermediate, pB, presumably is the biologically significant signaling state of the photoreceptor. Hence, significant structural rearrangements are expected to distinguish the pB state from the ground state, pG. The experimental findings so far have shown that the conformational changes in the pB state highly depend on the environment of the protein. In particular, millisecond and nanosecond time-resolved crystallography, probing the pB- (Genick et al., 1997a) and the pR state (Perman et al., 1998), as well as x-ray diffraction of a cryo-trapped pre-pR state (Genick et al., 1998), showed very little structural rearrangements outside the chromophore binding pocket.

In contrast, thermodynamic studies of PYP in solution indicated large heat capacity changes associated with pB formation and decay, consistent with significant structural rearrangements when pB is formed (Van Brederode et al., 1996; Hoff et al., 1999). The observed deviation from Arrhenius behavior of the pB→pG transformation kinetics was argued to be due to changes in heat capacity, ΔC_p, e.g., because it was found to be independent of pH (Hoff et al., 1999). It was estimated that 6200 $Å^2$ hydrophobic surface is

Submitted July 9, 2001, and accepted for publication November 26, 2001.

Address reprint requests to Dr. Klaas J. Hellingwerf, Laboratory for Microbiology, Nieuwe Achtergracht 166, 1018 WV Amsterdam, The Netherlands. Tel.: 31-20-5257055; Fax: 31-20-5257056; E-mail: k.hellingwerf@science.uva.nl.

0006-3495/02/03/1632/12 $2.00

exposed upon formation of pB (Hoff et al., 1999). However, it cannot be excluded that temperature dependence of ΔS and/or ΔH (not correlated with ΔC_p) in the transition between pB and pG contribute to the curved Arrhenius plots (Karplus, 2000).

FTIR difference spectroscopy of the amide region also provided evidence for global conformational changes in PYP (Hoff et al., 1999; Xie et al., 1996, 2001; Brudler et al., 2001). Furthermore, light-induced hydrogen-deuterium exchange measurements using FTIR spectroscopy and mass spectrometry showed that 23% of the amide groups, that were buried in pG, become solvent exposed in the pB state (Hoff et al., 1999).

An NMR study of PYP in solution indicated that the structure of the pB state was disordered to a significant degree (Craven et al., 2000). The apparent discrepancy between the crystallographic studies and the studies on PYP in solution was resolved when it was shown with FTIR spectroscopy that the size of the signals reflecting structural rearrangements in pB-pG difference spectra were strongly decreased in crystalline PYP (Xie et al., 2001).

Recently it was argued that the unfolded nature of the pB state resembles a molten globule state (Lee et al., 2001). Their conclusion was based on 1) measurement of the quenching of fluorescence emission from the single tryptophan in PYP, 2) analysis of the binding of the hydrophobicity probe ANS in the pB state, and 3) on circular dichroism spectroscopy measurements. These authors demonstrated that after accumulating the pB state by continuous illumination in the presence of ANS, a decay of the ANS fluorescence intensity could be fitted with a single rate constant reflecting subsequent recovery of pG (Lee et al., 2001). However, no measurement was made of the rate of formation of the signal, fluorescence spectra could not be recorded due to overlap of the ANS excitation and PYP (pG) absorption wavelengths, and the site of ANS binding was not localized.

The heat capacity change upon formation of pB has been determined to be -2.35 kJ mol^{-1} K^{-1}, consistent with the exposure of hydrophobic groups in this state (Van Brederode et al., 1996; Hoff et al., 1999). The transiently exposed hydrophobic site may be important for protein-protein interactions during biological signaling. Recently, the heat capacity change upon formation of pB was determined to be -0.1 kJ mol^{-1} K^{-1} in a PYP mutant where the 25 N-terminal residues were deleted (van der Horst et al., 2001). This indicates that the N-terminal domain is involved in the exposure of hydrophobic groups.

An NMR study on hydrogen-deuterium exchange differences between dark and light-activated PYP recently showed that the core of PYP in the pB state remains protected, whereas two regions including the N-terminal residues 6 to 18 and 26 to 29, become significantly perturbed (Craven et al., 2000). Based on the experimental evidence these authors propose a model for the structure of pB involving an equilibrium between an ordered and a partially unfolded state with strong perturbations in the 28 N-terminal residues.

PYP has two hydrophobic cores. The larger of these contains the chromophore-binding pocket, whereas the smaller one is formed by the two N-terminal α-helices and the central β-sheet (Borgstahl et al., 1995). It was put forward and recently proven that the partial unfolding of the N-terminal residues could account for most of the heat capacity change observed in solution (Craven et al., 2000; van der Horst et al., 2001). On the other hand, it has recently been pointed out that the chromophore environment is highly hydrophobic, and that the formation of a buried charge on Glu-46 drives the conformational changes in the pB state (Xie et al., 2001). Because, the chromophore in its *cis* configuration is oriented toward the external medium in pB, also the surface of the chromophore-binding pocket (with a low dielectric constant) is likely to become solvent exposed in the pB state. Which of the two hydrophobic cores transiently exposes the largest hydrophobic contact surface still remains to be determined.

Nile Red (NR) is a fluorescent probe that is very sensitive to the local polarity (i.e., its dielectric environment) and can be used to probe hydrophobic surfaces in proteins (Sackett and Wolff, 1987). In a polar environment NR has a low fluorescence quantum yield, whereas in more hydrophobic environments its quantum yield increases and its emission maximum becomes progressively blue shifted (Hou et al., 2000; Dutta et al., 1996).

Here we have used the fluorescent probe NR to probe the exposure of hydrophobic contact surface during the PYP photocycle in solution. Using this approach we were able to obtain kinetically resolved measurements that allowed comparison of the photocycle kinetics and the kinetics of structural rearrangements. We were also able to make a distinction between the two hydrophobic sites likely to become exposed in pB.

METHODS AND MATERIALS

Materials

Recombinant wild-type apoPYP was produced heterologously in *Escherichia coli*, as described previously (Kort et al., 1996). For an N-terminally truncated PYP derivative (Δ25-PYP) residues 1 to 25 were deleted using molecular genetic techniques (van der Horst et al., 2001). Both wild type and Δ25-apoPYP were reconstituted with the 1,1′-carbonyldiimidazole derivative of *p*-coumaric acid. This reagent was prepared by dissolving *p*-coumaric acid and 1,1′-carbonyldiimidazole (both at a concentration of 250 mM) in dry *N*,*N*-dimethylformamide and subsequently stirring the mixture overnight at 4°C (adapted from: Genick et al., 1997b; Imamoto et al., 1995). The reconstituted wild type and Δ25-holoPYP were used without removal of their genetically introduced hexa-histidine containing N-terminal tag.

Sample preparation

PYP samples (2 μM) were prepared in buffers of pH 4.0, 5.0, 6.0, 7.0, 8.0, and 9.0, i.e., 10 mM formic acid, 10 mM citric acid, 10 mM 2-(*N*-morpholino)ethanesulfonic acid, 10 mM potassium phosphate, 10 mM Tris/HCl, and 10 mM boric acid, respectively. Stock solutions of NR ranging in concentration from 1 to 100 μM were prepared in dimethylsulphoxide. Measurements were started 30 s after adding 20 μl of one of the NR stock solutions. Because of this procedure all samples contain 1% (v/v) dimethylsulphoxide. It was necessary to use this procedure because of aggregation and slow adsorption of NR to the walls of the cuvet, resulting in a steady decrease of the concentration of NR in the aqueous solution (Sackett and Wolff, 1987). We have tested the stability of NR fluorescence and absorption under our experimental conditions at pH 8.0 and found no changes within the first 10 min after dilution of NR in to the aqueous solutions. Consequently, all experiments with NR have been performed within the first 10 min after adding NR.

Steady-state fluorescence analyses

For the steady-state fluorescence analyses an AMINCO Bowman Series 2 Luminescence Spectrometer (Thermo Spectronic, Rochester, NY) was used. The excitation wavelength was set at 540 nm (bandpass, 16 nm), and the emission was recorded from 555 to 800 nm (bandpass, 4 nm) at a rate of 2 nm/s. To produce a steady-state mixture of pG and pB in the PYP sample a 462-nm light-emitting diode (LED) (full width at half maximum (FWHM), 22 nm) was used to continuously illuminate the sample. The percentage of accumulated pB was pH dependent and ranged from $\pm$25% for neutral pH to $\pm$85% at pH 4.0, which is consistent with a previous study (Hendriks et al., 1999a).

The fluorescence quantum yield of NR in 10 mM Tris/HCl buffer (pH 8.0) with and without the presence of PYP was determined by comparing its fluorescence to that of rhodamine-101 in ethanol ($\Phi_{fl} = 1$ (Eaton, 1988; Karstens and Kobe, 1980)). Both were excited at 540 nm with equal absorption at that wavelength.

Time-resolved (millisecond/second) fluorescence spectroscopy

To monitor the time-dependence of the release of NR from PYP the same spectrofluorimeter was used as for the steady-state measurements but now with the excitation wavelength set at 530 nm (bandpass, 16 nm), whereas the emission was monitored at 600 nm (bandpass, 4 nm) with a time resolution of 10 ms (a faster time resolution resulted in an unacceptably low signal to noise ratio). Samples were flashed with a photo flashlight (500-μs pulse-width), through a 400-nm long-pass filter, 10 s after the start of the measurement.

Steady-state and transient (millisecond/second) UV/Vis measurements

The actual concentration of PYP in the samples and the amount of pB that is formed upon flash and/or continuous illumination was measured with an HP 8453 UV/Vis diode array spectrophotometer (Hewlett-Packard Nederland BV, Amstelveen, NL) under similar geometric and illumination conditions as the fluorescence measurements described above. Spectra were collected from 210 to 800 nm with a time resolution of 100 ms.

Laser-flash photolysis spectroscopy

To study details of the NR-binding step we used an Edinburgh Instruments Ltd. LP900 spectrometer (Livingston, West Lothian, UK), equipped with both a CCD camera and a photomultiplier, in combination with a Continuum Surelite OPO laser (for further details, see Hendriks et al., 1999b). Although this setup is optimized for transient UV/Vis spectroscopy, it can also be used to measure emission spectra. The latter were measured with the CCD camera, using an integration time of 500 μs. The PYP sample was excited with 446-nm laserflashes of 7 to 8 mJ (pulse width 6 ns). The NR probe was excited with a 517-nm LED (FWHM, 40 nm) that continuously illuminated the sample. Emission was measured between 550 and 815 nm. For comparison, UV/Vis time traces were measured using the photomultiplier. To study the transition of pR to pB, traces were recorded at 500 nm, a wavelength at which selectively the presence of the pR intermediate can be monitored (Hoff et al., 1994). Additionally, traces were recorded at 468 nm to also be able to monitor pG recovery. These experiments were carried out with 1 μM NR and 10 μM PYP in 10 mM Tris/HCl, pH 8.0.

Analysis of steady-state fluorescence emission data

To be able to relate the fluorescence emission data with the amount of NR present in bound and nonbound form, it is important to be able to fit the shape of the overlapping emission peaks accurately. We found that a single Gaussian, Lorentzian, or Voigt function did not give satisfactory fits. Therefore, we designed a new function consisting of multiple Gaussians (multiGauss; see Eq. 1) that does give a satisfactory fit (see Fig. 1 *a*).

$$
\begin{aligned}
y &= B + \sum_{i=0}^{n-1} A(i, s_1) \cdot \exp\left[-\frac{1}{2}\left(\frac{x - x_c(i, s_2)}{w(i, s_3)} \right)^2 \right] \\
A(i, s_1) &= A_0 \cdot \exp(-s_i \cdot i) \\
x_c(i, s_2) &= x_c + s_2 \cdot i \\
w(i, s_3) &= w + s_3 \cdot i
\end{aligned}
\tag{1}
$$

In this equation, B is a baseline correction, n is the number of Gaussians, A is the amplitude, w is the width in cm^{-1}, x_c is the peak maximum in cm^{-1}, and s_1, s_2, and s_3 are factors to convert A, w, and x_c for the $i = 0$ Gaussian into the corresponding values for the $0 < i < n$ Gaussians. A value of 3 for n provided proper fits (Fig. 1 *a*) and was used throughout the analysis. In the analysis, first the spectra obtained from samples without PYP added were fitted with one multiGauss function to obtain the emission peak shape of NR in aqueous solution. Next, the spectra from samples containing pB were fitted with two multiGauss functions, one for the NR emission from aqueous solution (using the previously determined peak shape), and a second, to fit the emission of NR when bound to pB. This procedure was applied for each pH value separately. In the further analysis two assumptions were made: 1) that the quantum yield of NR is constant in the pH range from 4 to 9; and 2) that the amount of NR bound to the pG-state of PYP is negligible. Tests and literature have confirmed that these assumptions are allowable (data not shown; Sackett and Wolff, 1987).

Using these assumptions it is possible to convert the emission peak area into the corresponding concentration of NR, using one conversion factor for NR in aqueous solution and one for NR bound to pB, for all the measured data at different pH values. With this procedure the concentrations of NR (free and bound to pB) are directly determined from the emission spectra, thereby circumventing any errors that are introduced during sample preparation, allowing a more accurate comparison between the experiments performed at the different pH values.

Analysis of transient fluorescence emission data

The same data analysis procedure was used for the transient fluorescence emission data as for the analysis of the steady-state fluorescence data

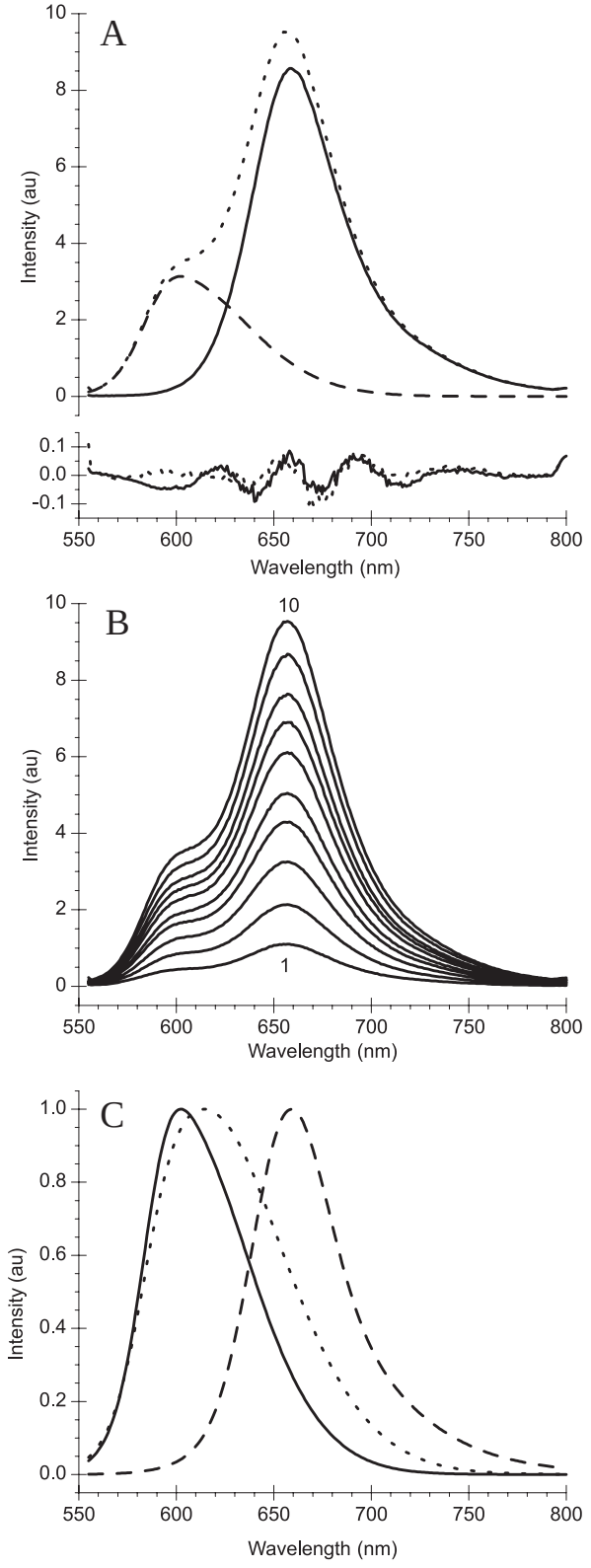

FIGURE 1 Fluorescence emission of Nile Red bound to the pB intermediate of PYP. (*A*) Emission spectra at pH 5.0, with excitation at 540 nm, of NR in the presence of buffer (similar to NR emission in the presence of PYP in the pG state; *solid line*), and in the presence of a steady-state mixture of pG and pB (0.3/0.7; *dotted line*). The dashed line was obtained via deconvolution and represents the pB-specific NR emission. The residuals after fitting with the multiGauss function (Eq. 1) are shown for the pG (*solid line*) and the steady-state mixture of pG and pB (*dotted line*) experiments. (*B*) NR concentration dependence of the emission spectrum in a PYP sample at pH 5.0 containing a steady-state mixture of pG and pB (0.3/0.7). Spectra are shown for NR concentrations from 100 nM NR (1) to 1 μM NR (10). (*C*) Representative deconvoluted emission spectra at pH 5.0 of NR in buffer (*dashed line*) and bound to pB (*solid line*). The dotted line is the deconvoluted pB-associated NR emission spectrum at pH 4.0, which is the only one that deviates significantly of the data obtained in the pH range from 4 to 9.

described above. However, to be able to correct for differences in NR concentration, introduced during sample preparation, an additional assumption had to be made. The ratio between the factors to convert emission peak area to concentration of NR (for the two types of NR emission) is the same for the two experimental set-ups, i.e., the LP900 transient (fluorescence) spectrometer and the AMINCO Bowman Series 2 Luminescence Spectrometer.

RESULTS

Steady-state and millisecond time-resolved measurements

To detect possible differences in structure between the pG and pB state of PYP the fluorescent hydrophobicity probe NR was used to assay binding of this probe to PYP. The absorption band of NR in water (589 nm) is considerably red shifted with respect to the absorption maximum of PYP (446 nm) and does not significantly overlap with, nor interfere with, the absorption by PYP. This makes NR an ideal candidate as a probe for conformational transitions in PYP. The emission characteristics of NR in aqueous solution and in the presence of PYP, when the protein is in its pG state, are the same within the error of the measurement (quantum yields of 0.02 and 0.026, respectively). Also no change in peak maximum, spectral shape, or quantum yield is observed between pH 4 and 9 for NR fluorescence. From this it was concluded that binding of NR to the pG state of PYP is negligible.

However, when the pB intermediate was accumulated, by continuous illumination with blue light, a new fluorescent species was observed (see Fig. 1 *A*). The emission maximum of this species was at 600 nm, strongly blue shifted with respect to the NR emission in aqueous solution (659 nm), indicating that an environment with low dielectric constant is sensed by the probe, when bound to the pB state of PYP. Identical observations were made with reconstituted wt-PYP after removal of the N-terminal hexa-histidine containing tag by proteolysis with enterokinase.

Deconvolution of the emission spectrum into emissions resulting from NR in aqueous solution and NR bound to PYP provides us with some of the emission characteristics of NR bound to the pB state of PYP (dashed line in Fig. 1 *A*). Like the emission of NR in aqueous solution, the shape of the emission from NR bound to pB can be fitted

well with a multiGauss function (see Eq. 1 and Materials and Methods).

The recovery of pG from pB can be followed by monitoring the fluorescence of NR at 600 nm on a millisecond time-scale, either after discontinuing continuous blue light illumination or after flash-excitation of PYP. This was done at a pH ranging from 4 to 9. The observed recovery kinetics were slightly slower compared with those found in parallel UV/Vis spectroscopy experiments (data not shown).

Nile Red titrations

It was not possible to saturate the binding of NR to pB due to low solubility of NR (Sackett and Wolff, 1987) in combination with a relative low affinity for PYP. However, it was possible to determine the equilibrium-binding constant (K_B) of NR to pB at pH 4.0, 5.0, 6.0, 7.0, 8.0, and 9.0. To determine K_B, the emission spectrum of NR in the presence of a steady-state mixture of pG and pB was measured at several NR concentrations ranging up to 1 μM, which is close to the solubility limit of NR in aqueous solution. A typical set of results (obtained at pH 5.0) is shown in Fig. 1 *B*. From these fluorescence emission data K_B values were determined using Eq. 2, which describes the association/dissociation equilibrium between the pB form of PYP and Nile Red.

$$\begin{aligned} &NR_{free} + pB_{free} \underset{k_2}{\overset{k_1}{\rightleftharpoons}} NRpB \\ &K_B = \frac{[NRpB]}{[NR_{free}] \cdot [pB_{free}]} \\ &[pB_{total}] = [NRpB] + [pB_{free}] \\ &[NR_{total}] = [NRpB] + [NR_{free}] \end{aligned} \quad (2)$$

The concentration of NR bound to pB ([NRpB]) and the amount of NR in aqueous solution ([NR_{free}]) was obtained via a fit of the emission spectra with multiGauss function(s) (see Eq. 1 and Materials and Methods). The total amount of NR added [NR_{total}] is obtained by adding [NRpB] and [NR_{free}]. The total amount of pB formed [pB_{total}] was determined separately in a parallel UV/Vis experiment under similar experimental conditions as the fluorescence measurements. The concentration of free pB ([pB_{free}]) was then obtained by subtracting [NRpB] from [pB_{total}]. The shapes of the peaks that were fitted to the emission spectra are shown in Fig. 1 *C*. The peak shape of the aqueous NR emission is independent of pH within the pH range studied. The shape of the pB-associated NR emission showed a negligible pH dependence (data not shown) with the exception of pH 4.0 where the emission has a much broader spectrum and is shifted slightly to the red (λ_{max} = 614 nm).

In Fig. 2 *A* the NR titration data is summarized and plotted in such a way that the slopes of the lines equal the K_B. From this plot it is evident that K_B is pH dependent. This is shown more clearly in Fig. 2 *B* where the K_B is plotted as a function of pH. The obtained pH profile suggests that a fit of this data would require at least two pK_a values, one at ~5.5 and the other at 9 or higher.

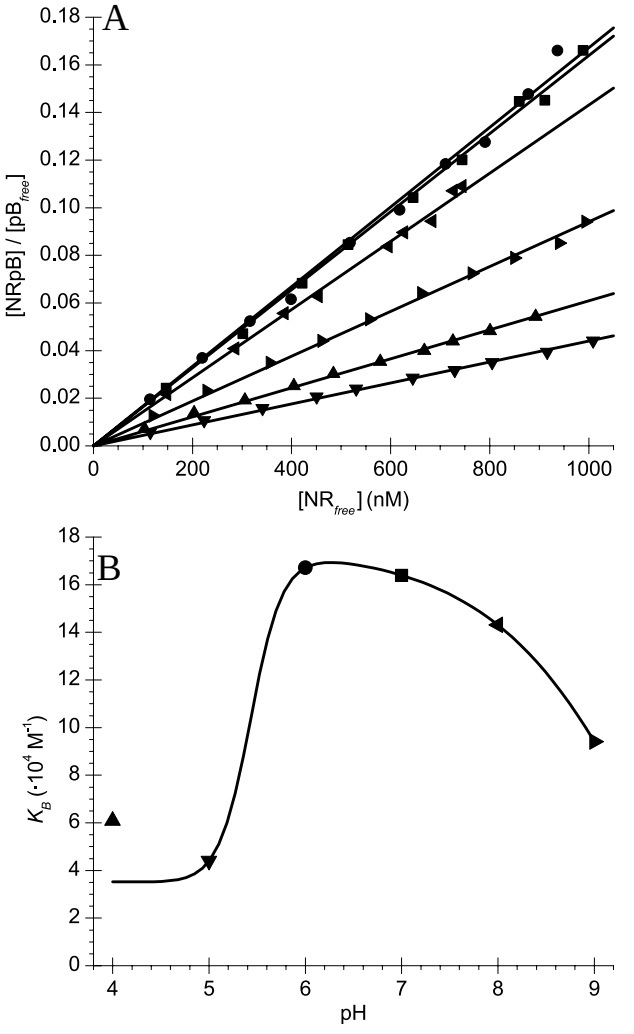

FIGURE 2 Quantitative analysis of NR binding to the pB-intermediate of PYP. (*A*) Determination of the NR binding constant K_B at pH 4.0 (▲), pH 5.0 (▼), pH 6.0 (●), pH 7.0 (■), pH 8.0 (◀), and pH 9.0 (▶). Data are plotted so that the slope of each line equals K_B (deduced from Eq. 2). (*B*) pH dependence of the binding constant K_B. A proposed fit with the Henderson-Hasselbalch equation using the pK_a values of 5.5 (n = 3) and 10 (n = 0.5) is included.

From the titration data it was derived that, compared with NR in aqueous solution, the pB-associated NR emission peak area was ~5.8 times larger for the same concentration of NR. Assuming that the extinction coefficient does not change significantly upon binding to PYP we calculated that the fluorescence quantum yield for pB-associated NR was 0.12.

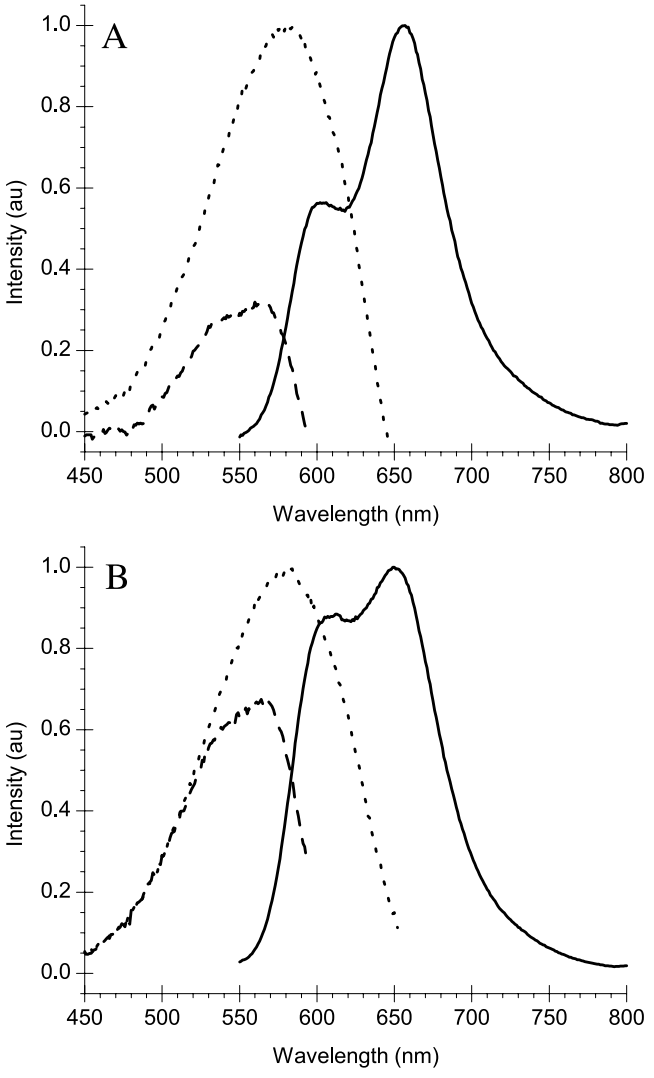

FIGURE 3 Steady-state excitation- and emission spectra of NR in a steady-state mixture of pG and pB of wild-type PYP and Δ25-PYP. (*A*) Fluorescence excitation spectra of NR with detection at 600 nm (*dashed line*) and 659 nm (*dotted line*), selective for pB-associated NR and free NR respectively, in the presence of a steady-state mixture of pG and pB (0.7/0.3) of wild-type PYP at pH 8.0. The emission spectrum (*solid line*) was recorded with excitation at 540 nm. (*B*) Fluorescence excitation- and emission spectra for a steady-state mixture of pG and pB (0.1/0.9) of Δ25-PYP at pH 8.0.

Analysis of truncated Δ25-PYP

From NMR-measurements (Craven et al., 2000) and UV/Vis kinetic absorption measurements (Van Brederode et al., 1996; van der Horst et al., 2001), both in solution, it is clear that a large structural change occurs in PYP upon formation of the pB state, particularly in its N-terminal domain. This N-terminal domain is therefore a prime candidate for the location of a NR binding site. However, when we studied NR emission in the presence of the Δ25-PYP mutant, in which the N terminus is deleted (residues 1–25), we did not detect any NR binding to the pG state of Δ25-PYP. Also, we observed the same shift in fluorescence emission from NR, upon formation of the pB intermediate of Δ25-PYP, as was found for wt-PYP (see Fig. 3). In Fig. 3 *A* the NR excitation and emission spectra of a steady-state pG/pB mixture of wild-type PYP is shown. Two excitation spectra are presented, one with the emission monitored at 600 nm (reflecting emission from pB-associated NR; dashed line) and one with the emission monitored at 659 nm (reflecting emission from free NR; dotted line). These excitation spectra were normalized with respect to the maximum of the included emission spectrum keeping the relative peak heights between the two excitation spectra intact. Fig. 3 *B* shows the equivalent data for Δ25-PYP. Note that in the Δ25-PYP sample more pB was accumulated, which explains the increased pB-associated NR emission. Otherwise the excitation and emission spectra were identical. Additionally, an NR titration experiment was performed with Δ25-PYP at pH 5.0 and 8.0. The obtained NR binding constants were similar to those found for wild-type PYP (see Table 1), indicating that the observed pH dependence of the NR binding constant in wild-type PYP is also present in Δ25-PYP.

TABLE 1 Nile Red to pB binding constants

pH	K_B for wild-type PYP ($\cdot 10^4$ M^{-1})	K_B for Δ25-PYP ($\cdot 10^4$ M^{-1})
4.0	6.09 ± 0.04	
5.0	4.40 ± 0.03	10.2 ± 0.1
6.0	16.7 ± 0.2	
7.0	16.4 ± 0.1	
8.0	14.3 ± 0.1	17.0 ± 0.2
9.0	9.41 ± 0.08	

Determination of the Nile Red to pB binding constants for wild-type PYP is presented in Fig. 2.

pB_{dark} state and the free chromophore

To determine if the acid-induced pB-state, pB_{dark} (Hoff et al., 1997), is structurally similar to the light-induced pB state, the NR emission spectrum of a wild-type PYP sample at pH 1.8 was determined. At this pH PYP is largely in the pB_{dark} state, a state with similar UV/Vis spectral properties as pB, but which is formed due to the low pH and not due to illumination of the sample. NR in aqueous solution at this low pH still has the same characteristics as in the pH range of 4 to 9 except for a lower emission intensity, which may either be caused by a decreased solvability or a change in quantum yield. In the presence of pB_{dark} the NR emission spectrum was similar but not identical to those observed in a steady-state mixture of pG and pB at a pH ranging from 4 to 9. Two different NR emission bands were observed. However, the pB_{dark}-associated NR emission has its maximum at 632 nm, which is clearly red shifted from the

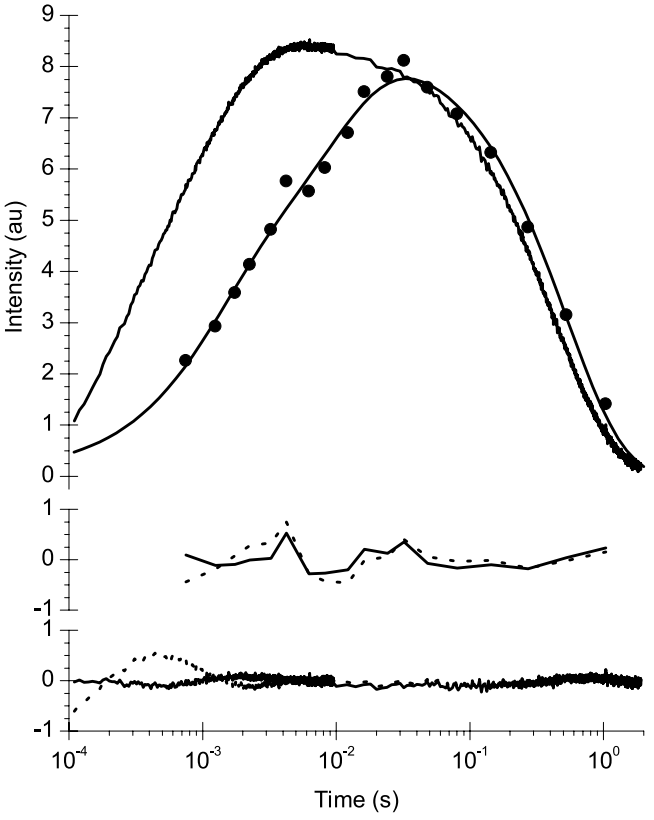

FIGURE 4 Comparison of photocycle kinetics determined via NR-emission and UV/Vis absorption. Two types of data are shown, a UV/Vis absorption time trace monitored at 468 nm and the amount of NR bound to the pB state of PYP at discrete time points, with a curve fitted through the data points. The data were normalized via the contributions of the recovery exponent obtained in the exponential fit of the data. Both types of data were recorded on the same set-up and with the same amount of PYP and NR present at pH 8.0. Below are the residuals obtained using a monoexponential fit ($\chi^2_{NR} = 1.2 \cdot 10^{-5}$; $\chi^2_{abs} = 9.1 \cdot 10^{-7}$; *dotted line*) and a biexponential fit ($\chi^2_{NR} = 6.8 \cdot 10^{-6}$; $\chi^2_{abs} = 2.0 \cdot 10^{-7}$; *solid line*) of the rise component.

emission maximum at 600 nm for the pB-associated NR emission.

As a control, the NR emission was also determined in the presence of the free chromophore *p*-coumaric acid (dissolved at 2 μM), both at pH 6.0 and 9.0. Under those conditions the NR emission did not change noticeably with respect to the NR emission in aqueous solution (data not shown), indicating that the pB-associated NR emission is not due to binding to the chromophore, which becomes exposed in pB.

Nile Red emission and PYP absorption kinetics

Kinetic measurements of the changes in pB-associated NR emission were compared with changes in UV/Vis absorption of PYP. At pH 8.0 both the formation of pB-associated NR emission, as well as its subsequent disappearance, was analyzed using laser-flash transient fluorescence spectroscopy. Emission spectra were recorded with delays ranging from 500 μs to 1.04 s. In Fig. 4 the peak areas of pB-associated NR emission and a transient absorption trace at 468 nm are presented. The two data sets were scaled using the amplitude of the single decay component, reflecting pG recovery, obtained in the fitting procedure.

The pB-associated NR emission was fitted with two rise-components, in addition to a single decay component (Table 2). Using a single rate constant for fitting of the rise of the pB-associated NR emission gave unsatisfactory results, suggesting pB associated NR emission at time 0. It was estimated from the Stokes-Einstein relation that in the diffusion-limited case a 200-μs time constant would be expected for our experimental conditions. Because the fastest time constant observed for the fluorescence rise was 1.2 $\pm$ 0.7 ms (with an amplitude of 0.43), these results suggest that the measurements were not diffusion limited and reflected the kinetics of structural rearrangements.

For comparison the photocycle kinetics of PYP in the presence of NR were determined by measurement of transient absorption changes at 468 nm of the same samples used for NR fluorescence (Fig. 4; Table 2). This allowed direct comparison between the NR fluorescence and the photocycle kinetics. The presence of NR did not influence the photocycle kinetics. As for the NR emission, two components were necessary to fit the rise phase at 468 nm in agreement with a previous study (Hoff et al., 1994). The value of the two rise components in the absorption data were determined at 500 nm, because it is not possible to get an accurate fit of these two rise components at 468 nm. Note that the formation of the pB-associated NR emission is about eight times slower than pB formation measured by UV/Vis absorption spectroscopy. Also, the decay of pB-associated NR emission is slightly slower (~30%) than the decay at 468 nm, reflecting recovery of the pG state. The differences between the NR fluorescence and photocycle kinetics (Fig. 4; Table 2) were consistently detected and well within the accuracy of our experiments.

TABLE 2 Comparison of the Nile Red emission and UV/Vis absorption kinetic constants

Type of data	τ_1 (Amplitude)	τ_2 (Amplitude)	τ_3 (Amplitude)
NR emission	1.2 $\pm$ 0.7 ms (0.43)	10 $\pm$ 2 ms (0.57)	530 $\pm$ 40 ms (−1)
UV/Vis absorption	213 $\pm$ 9 μs (0.48)	1.23 $\pm$ 0.02 ms (0.52)	405 $\pm$ 1 ms (−1)

The Nile Red emission and UV/Vis absorption kinetics were fitted from the flash-photolysis data presented in Fig. 4.

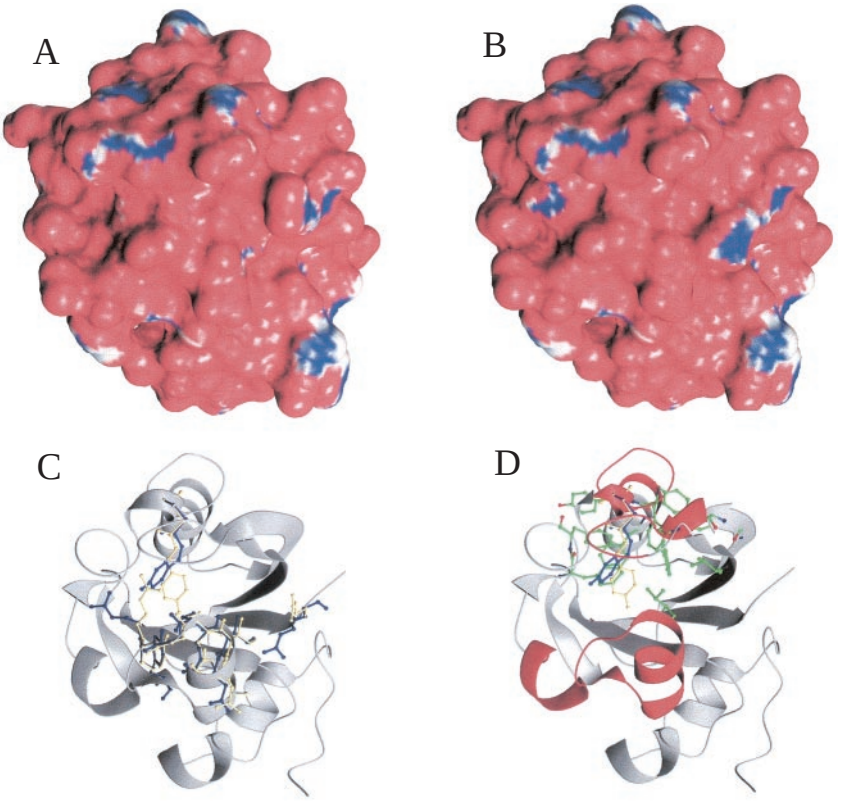

FIGURE 5 Hydrophobicity analysis of the crystal structures of pG and pB. (*A*) GRID analysis showing the hydrophobicity of the solvent-accessible molecular surface (calculated with a 1.4-Å probe) of the crystal structure coordinates of the pG state (*blue*, hydrophobic). (*B*) GRID analysis showing the hydrophobicity of the solvent-accessible molecular surface of the crystal structure coordinates of the pB state (*blue*, hydrophobic). (*C*) Secondary structure representation of PYP, with chromophore and protein (residues 42, 45–52, and 124) coordinates shown for atoms that showed conformational change in the crystalline pB state (*blue*) relative to the crystalline pG state (*yellow*). (*D*) Proposed binding site for Nile Red of PYP in solution in the pB state. The secondary structure representation of residues 42 to 58, 69 to 78, and 95 to 100, that show conformational changes in addition to the N-terminal domain in solution NMR experiments (Craven et al., 2000) are shown in red. The proposed binding site for Nile Red (consisting of some or all of the residues F62, F63, F75, Y76, F79, F92, Y94, F96, V107, and V120) is shown (with carbon atoms in *green*). The structure coordinate file deposited at the Protein Data Bank (Berman et al., 2000) (http://www.rcsb.org/pdb) with PDB ID: 2PYP (Genick et al., 1997a) was used to prepare the images. All images have the same orientation. Figures were drawn with Aesop (M. Noble, unpublished).

DISCUSSION

The possible exposure of a hydrophobic surface upon formation of the pB intermediate in the photocycle of PYP has been suggested on the basis of time-resolved absorption experiments (Meyer et al., 1989) and was later also implied on the basis of specific heat capacity changes derived from time-resolved absorption measurements (Van Brederode et al., 1996), transient proton uptake and release (Meyer et al., 1993; Hendriks et al., 1999a), and binding to lipid bilayers (Salamon et al., 1995). However, this view became heavily debated upon publication of a crystal structure of the pB intermediate (Genick et al., 1997a), which does not show a structural change that would suggest such an exposure of a hydrophobic surface. Meanwhile FTIR experiments have shown, in a direct comparison of the two PYP forms (i.e., in aqueous solution and in a crystalline lattice), that the behavior of PYP in crystals is different from that in solution with respect to global structural changes (Xie et al., 2001). In this study we have further characterized the exposure of a hydrophobic surface in pB with the aid of the fluorescent hydrophobicity probe NR.

Recently it was put forward that the pB state resembles a molten globule state (Lee et al., 2001). One of their observations was a 12% increase of the fluorescence of the hydrophobicity probe ANS in the pB state, compared with the pG state. No binding site was suggested, however, and no kinetic analysis of the exposure of the ANS binding site was performed. Because ANS binds to the pG state and excitation of ANS also excites the PYP photocycle, the analysis presented here would not be possible using the ANS probe.

The excitation maximum of Nile Red is sufficiently distant from the absorption maximum of the pG state of PYP to allow the probe to be used under conditions of continuous excitation of NR, without inducing photochemistry in PYP. From the steady-state emission spectra of NR in buffer, in the presence of pG, and in the presence of a steady-state mixture of pB and pG (see Fig. 1 *A*) we can deduce that NR only binds to pB and not to pG. The association of NR with pB was further shown by comparing time-resolved NR emission and UV/Vis absorption measurements on a millisecond to second time scale, where the pG recovery kinetics were similar for both types of experiment. To determine if the transient binding of NR to pB could be explained by hydrophobicity changes on the surface of the known pB crystal structure, we analyzed the surface hydrophobicity of the pG and the pB crystal structure using GRID (Goodford, 1985). We did not observe a significant difference in surface hydrophobicity (see Fig. 5, *A* and *B*), indicating that we are indeed looking at a structural change specific for PYP in solution. A representation of the differences between the pG and pB crystal structure is shown in Fig. 5 *C*.

The sensitivity of NR emission to the polarity of the environment can be understood from the internal charge

transfer in the excited state and its stabilization by a geometrical change of the NR molecule in the excited state in polar solvents. Such a state is called a twisted internal charge transfer state (Dutta et al., 1996). It has been shown that a twisted internal charge transfer state is characterized by red-shifted absorption and emission maxima and a low fluorescence quantum yield. This is in good agreement with the experimental fluorescence properties of NR in solvents with different dielectric constants (Dutta et al., 1996; Sackett and Wolff, 1987; Ghoneim, 2000; Greenspan and Fowler, 1985; Sarkar et al., 1994; Datta et al., 1997), where the fluorescence emission maximum (λ_{fl}) is positively correlated and the fluorescence quantum yield (Φ_{fl}) is negatively correlated to the dielectric constant or the dielectric polarity of the solvent. For two proteins (κ-casein and albumin) this correlation between the fluorescence emission maximum and the fluorescence quantum yield of protein-bound NR has also been established (Sackett and Wolff, 1987). From the fluorescence maximum of the pB-associated NR emission observed in this study a dielectric constant of $D = 15$ to 20 is expected for the environment of NR near its binding site. The fluorescence quantum yield of the pB-associated NR (0.12), however, is a factor of two smaller than expected from these correlations. It is proposed that the reduced fluorescence quantum yield is due to specific quenching of NR fluorescence by the surrounding PYP molecule.

By titrating NR it was intended to determine the binding constant K_B as well as the number of NR molecules that bind to a single PYP molecule in the pB state. However, due to the low solubility of NR (Sackett and Wolff, 1987) and its relatively low affinity for PYP, we were not able to saturate binding of NR to the pB state of PYP. As a result, we were not able to determine the number of NR molecules binding to PYP in the pB state. However, based on the molecular dimensions of NR and PYP, it is likely that they bind in a one-to-one stoichiometry.

The pH dependence of the determined binding constants indicates that a fit of the data would require at least two pK_a values (one around 5.5 and one around 9 or higher). In a previous study that also looked at structural changes upon formation of pB, which used transient proton uptake and release as a probe (Hendriks et al., 1999a), pK_a values of 5.5 and 10 were observed. These pK_a values were fit onto the pH dependence of K_B using the Henderson-Hasselbalch equation, which resulted in a good fit (see Fig. 2 *B*). Note, that a pK_a value of 9 instead of 10 also provides a good fit through the data. A pK_a of ~6.4 has also been found in titrations of several properties of the pB state (Genick et al., 1997b; Demchuk et al., 2000). However, it was not possible to fit a pK_a of 6.4 onto the data presented here.

The pB-associated NR emission spectrum also shows a pH dependence. The emission maximum of pB-associated NR emission at pH values of 4.0 and 1.8 is red shifted with respect to the emission maximum in the pH range from 5 to 9. This red shift can be interpreted as a more polar nature of the hydrophobic surface that NR binds to. Note that a change in emission maximum also implies a change in the quantum yield of NR emission. This possibly explains why the data point at pH 4.0 in Fig. 2 *B* deviates slightly from the fitted curve, because the analysis of the data did not take this effect into account. Note that the pH dependence of the K_B does not coincide with the pH dependence of the pB-associated NR emission maximum. In other words, the pH dependence of K_B is not caused by a change in polarity of the NR-binding site. It is therefore possible that the pH dependence of K_B is caused by a difference in the structure of pB. It already has been proposed that the pB state exists in multiple configurations, both ordered and partially unfolded (Craven et al., 2000). In light of the observed pH dependence of K_B we would like to propose that the equilibrium between these ordered and partially unfolded states is pH dependent. More specifically, at low pH the number of pB molecules with a structural change large enough to allow binding of NR is lower than at high pH. The apparent pK_a for this difference is ~5.5. Recently it was shown via FTIR spectroscopy that E46 is the driving force behind the structural change observed in pB. It is therefore possible that the pK_a of 5.5 observed in the pH dependence of K_B is caused by E46. Even though a pK_a of 6.4 has already been assigned to E46 on the basis of kinetic measurements (Demchuk et al., 2000), it is possible that in the partially unfolded form of pB, that is able to bind NR, E46 has a pK_a of 5.5. The pK_a of 6.4 determined for E46 is based on the pH dependence of the pG recovery reaction measured via UV/Vis absorption spectroscopy. Consequently, this pK_a represents the situation in a structural form of pB that is able to isomerize the chromophore and therefore able to recover to pG. It is likely that the structural form of pB that is able to isomerize the chromophore is a more ordered form, similar to the crystal structure of pB. This also explains the 10-fold faster recovery reaction for PYP in crystalline form (Xie et al., 2001), because the pB structures formed in a crystal will predominantly be able to isomerize the chromophore, whereas in solution many of the conformations pB adopts may be unable to do so.

To interpret the data more accurately it is important that we know the location of the NR binding site in PYP. Using the available information we can narrow down the location of this binding site. It is known that NR binds to hydrophobic parts of a protein (Sackett and Wolff, 1987). NR does not bind to the ground state of PYP, thus the NR binding site must be buried when PYP is in its ground state. PYP has two buried hydrophobic cores, the major hydrophobic core, which is also part of the chromophore-binding pocket, and the minor hydrophobic core shielded by the N-terminal part of the protein (Borgstahl et al., 1995). NMR experiments indicate that around both cores structural changes take place upon formation of pB (Craven et al., 2000). This provides us with two possible areas where NR may bind. By analyzing

the Δ25-PYP mutant, it is possible to distinguish between these two possible areas. The Δ25-PYP mutant has similar NR-binding characteristics as wild-type PYP. The most important similarity being that NR binds to pB and not pG. Therefore, it can be excluded that NR binds to the hydrophobic core shielded by the N-terminus in wild-type PYP. It also means, with respect to the results of van der Horst et al. (2001), that the phenomena of NR binding to the pB state of PYP and the non-Arrhenius behavior of the pB→pG recovery are caused by different structural protein changes (both involving exposure of hydrophobic surfaces and/or changes in its accessibility, though). After the argument that from the size of the heat capacity changes in wild-type PYP an exposure of 6200 $Å^2$ is expected (Hoff et al., 1999), the reduced value of the heat capacity change for the pB→pG transition of the Δ25-PYP truncation mutant would still allow the exposure of 250 $Å^2$, which is a sufficient binding-area for Nile Red, assuming a direct relationship between the measured value of ΔC_p and exposed hydrophobic surface area. It cannot be excluded that the curved Arrhenius plots are caused by a temperature dependence of ΔS and/or ΔH (not correlated with ΔC_p) in the transition between pB and pG (Karplus, 2000). In addition, changes in the accessibility of a hydrophobic site for Nile Red does not necessarily have to be correlated with a large increase of hydrophobic contact area.

The major hydrophobic core is left as the only area of the protein that potentially contains the NR binding site. NMR experiments have indicated that, besides the N-terminal domain, residues 42 through 58, 69 through 78, and 95 through 100, which encompass the chromophore-binding pocket and contain part of the major hydrophobic core, show structural changes upon formation of pB (Craven et al., 2000). A hydrophobicity analysis, using GRID (Goodford, 1985), of the molecular surface of the amino acid clusters 69 through 78 and 95 through 100 shows this region to represent a significantly hydrophobic site. Rearrangements of the clusters 69 to 78 and 95 to 100 such as expected from the NMR studies, could potentially result in solvent-exposure of a hydrophobic surface, consisting of some, or all of the residues F62, F63, F75, Y76, F79, F92, Y94, F96, V107, and V120. This site is also relatively close to the chromophore (see Fig. 5 *D*). Exposure of this site would not be expected to result in deprotection of the amide groups of these "core" residues.

The fluorescence emission maximum of pB-bound Nile Red is direct evidence for the hydrophobic nature of the interaction between pB and Nile Red. Because the photocycle kinetics are affected by solvent properties (Meyer et al., 1989), binding of Nile Red to the protein might cause changes in the photocycle. However, it was observed in control experiments that the presence of Nile Red did not significantly influence the spectral or kinetic characteristics of the photocycle.

The pB intermediate is predominantly assigned via UV/Vis spectroscopy. However, the visible color of PYP is sensitive only to the structure of the chromophore and its immediate environment. The large blue shift observed upon formation of pB in UV/Vis spectroscopy is mainly caused by the protonation of the chromophore. Thus by comparing a time-resolved UV/Vis experiment with a time-resolved NR-emission experiment, we are able to compare the kinetics of the protonation change of the chromophore with the kinetics of the exposure of a hydrophobic surface. From Fig. 4 it is evident that chromophore protonation precedes exposure of the hydrophobic surface probed by NR. The exposure of the hydrophobic surface is about eightfold slower than the protonation of the chromophore. Due to the restricted time resolution of our NR-emission experiment it was difficult to compare the UV/Vis absorption and NR-emission experiment in the submillisecond region. The experiment was therefore repeated using representative sample conditions on a different setup (Koeberg et al., 2001) with a better time resolution (100 μs) with essentially the same results. The delay between spectroscopic and structural transitions observed via NR binding is in agreement with time resolved FTIR data that also showed a delay between changes in the protonation state of the chromophore and structural changes in the protein backbone (Xie et al., 2001). The time constant for the absorption changes in the amide region associated with pB formation was reported to be 2 ms, which is slower than our NR fluorescence measurements (Table 2). We note that the experimental conditions, in particular the solvent conditions and protein concentration of the samples, differ between the FTIR- and the NR fluorescence experiments. Therefore, the kinetics cannot be directly compared. However, the delay of the structural changes in the pG→pB transition observed by FTIR spectroscopy is in agreement with our observations.

The optical transition from pR to pB consists of more than one component (Hoff et al., 1994). This was proposed to be due to heterogeneity of the pB state and/or its formation, in agreement with NMR, FTIR, and CD studies (Craven et al., 2000; Brudler et al., 2001; Lee et al., 2001). The bi- (or multi-) exponential nature of the NR binding phase can also be interpreted to reflect the structural heterogeneity of PYP in the pB state, consisting of both partially unfolded and more ordered forms of pB, as recently proposed (Craven et al., 2000). This interpretation is supported by the fact that no spectral evolution of the NR emission bound to pB is observed. NR bound at early and late times shows identical spectra, which indicates binding to the same site.

In addition to the temporal independence of chromophore protonation and the structural changes exposing a hydrophobic surface it was found that the reversion of those processes is also decoupled, namely the hydrophobic surface is still exposed after the chromophore has been deprotonated. These results show that the analysis of the action of photoreceptors by absorption spectroscopy only is not suf-

ficient and may lead to failure of detecting important structural changes as well as decisive kinetic steps. We have shown here that use of the fluorescent hydrophobicity probe NR (and related compounds) has a potential for revealing the existence of protein conformational states and kinetics of protein structural changes.

CONCLUSIONS

With the aid of the polarity-sensitive fluorescent probe NR we were able to determine that a hydrophobic surface is transiently exposed in PYP upon formation of its pB state. This surface was found not to include the N-terminal 25 residues but likely to become exposed near the chromophore binding pocket. NR specifically binds to the pB intermediate of PYP and not to its ground state. Also, the use of NR does not significantly influence the photocycle properties of PYP. Therefore NR seems to be an ideal probe to study the exposure of hydrophobic surface around the chromophore-binding pocket.

Further, we have shown that the binding constant of NR to pB is pH dependent, which possibly is caused by structural differences of pB at different pH values. Time-resolved measurements of the pB associated NR emission showed that the kinetics associated with the rise phase of the conformational changes are approximately 8 times slower than the transitions associated with formation of the pB state determined by UV/Vis spectroscopy. This implies that chromophore protonation precedes the exposure of hydrophobic surface. The results obtained in this study are consistent with structural heterogeneity of the pB state.

J. W. Verhoeven is gratefully acknowledged for making available equipment for time-resolved spectroscopy. This research was supported by the Netherlands Foundation for Chemical Research (CW) with financial assistance from the Netherlands Organization for Scientific Research (NWO), the Royal Dutch Academy of Science, and the Academy of Science of Nordrhein-Westfalen, and the Human Frontier Science Program Organization.

REFERENCES

Berman, H. M., J. Westbrook, Z. Feng, G. Gilliland, T. N. Bhat, H. Weissig, I. N. Shindyalov, and P. E. Bourne. 2000. The protein data bank. *Nucleic Acids Res.* 28:235–242.

Borgstahl, G. E., D. R. Williams, and E. D. Getzoff. 1995. 1.4-A structure of photoactive yellow protein, a cytosolic photoreceptor: unusual fold, active site, and chromophore. *Biochemistry.* 34:6278–6287.

Brudler, R., R. Rammelsberg, T. T. Woo, E. D. Getzoff, and K. Gerwert. 2001. Structure of the I1 early intermediate of photoactive yellow protein by FTIR spectroscopy. *Nat. Struct. Biol.* 8:265–270.

Craven, C. J., N. M. Derix, J. Hendriks, R. Boelens, K. J. Hellingwerf, and R. Kaptein. 2000. Probing the nature of the blue-shifted intermediate of photoactive yellow protein in solation by NMR: hydrogen-deuterium exchange data and pH studies. *Biochemistry.* 39:14392–14399.

Datta, A., D. Mandal, S. K. Pal, and K. Bhattacharyya. 1997. Intramolecular charge transfer processes in confined systems: nile red in reverse micelles. *J. Phys. Chem. B.* 101:10221–10225.

Demchuk, E., U. K. Genick, T. T. Woo, E. D. Getzoff, and D. Bashford. 2000. Protonation states and pH titration in the photocycle of photoactive yellow protein. *Biochemistry.* 39:1100–1113.

Dutta, A. K., K. Kamada, and K. Ohta. 1996. Spectroscopic studies of nile red in organic solvents and polymers. *J. Photochem. Photobiol. A Chem.* 93:57–64.

Eaton, D. F. 1988. Reference materials for fluorescence measurement. *Pure Appl. Chem.* 60:1107–1114.

Genick, U. K., G. E. Borgstahl, K. Ng, Z. Ren, C. Pradervand, P. M. Burke, V. Srajer, T. Y. Teng, W. Schildkamp, D. E. McRee, K. Moffat, and E. D. Getzoff. 1997a. Structure of a protein photocycle intermediate by millisecond time-resolved crystallography. *Science.* 275:1471–1475.

Genick, U. K., S. Devanathan, T. E. Meyer, I. L. Canestrelli, E. Williams, M. A. Cusanovich, G. Tollin, and E. D. Getzoff. 1997b. Active site mutants implicate key residues for control of color and light cycle kinetics of photoactive yellow protein. *Biochemistry.* 36:8–14.

Genick, U. K., S. M. Soltis, P. Kuhn, I. L. Canestrelli, and E. D. Getzoff. 1998. Structure at 0.85 A resolution of an early protein photocycle intermediate [see comments]. *Nature.* 392:206–209.

Ghoneim, N. 2000. Photophysics of Nile red in solution: steady state spectroscopy. *Spectrochim. Acta Part A Mol. Biomol. Spectrosc.* 56: 1003–1010.

Goodford, P. J. 1985. A computational procedure for determining energetically favorable binding sites on biologically important macromolecules. *J. Med. Chem.* 28:849–857.

Greenspan, P., and S. D. Fowler. 1985. Spectrofluorometric studies of the lipid probe, nile red. *J Lipid Res.* 26:781–789.

Hendriks, J., W. D. Hoff, W. Crielaard, and K. J. Hellingwerf. 1999a. Protonation/deprotonation reactions triggered by photoactivation of photoactive yellow protein from *Ectothiorhodospira halophila*. *J. Biol. Chem.* 274:17655–17660.

Hendriks, J., I. H. van Stokkum, W. Crielaard, and K. J. Hellingwerf. 1999b. Kinetics of and intermediates in a photocycle branching reaction of the photoactive yellow protein from *Ectothiorhodospira halophila*. *FEBS Lett.* 458:252–256.

Hoff, W. D., I. H. M. Van Stokkum, J. Gural, and K. J. Hellingwerf. 1997. Comparison of acid denaturation and light activation in the eubacterial blue-light receptor photoactive yellow protein. *Biochim. Biophys. Acta Bioenerget.* 1322:151–162.

Hoff, W. D., I. H. van Stokkum, H. J. van Ramesdonk, M. E. van Brederode, A. M. Brouwer, J. C. Fitch, T. E. Meyer, R. van Grondelle, and K. J. Hellingwerf. 1994. Measurement and global analysis of the absorbance changes in the photocycle of the photoactive yellow protein from *Ectothiorhodospira halophila*. *Biophys. J.* 67:1691–1705.

Hoff, W. D., A. Xie, I. H. Van Stokkum, X. J. Tang, J. Gural, A. R. Kroon, and K. J. Hellingwerf. 1999. Global conformational changes upon receptor stimulation in photoactive yellow protein. *Biochemistry.* 38: 1009–1017.

Hou, Y. W., A. M. Bardo, C. Martinez, and D. A. Higgins. 2000. Characterization of molecular scale environments in polymer films by single molecule spectroscopy. *J. Phys. Chem. B.* 104:212–219.

Imamoto, Y., T. Ito, M. Kataoka, and F. Tokunaga. 1995. Reconstitution photoactive yellow protein from apoprotein and *p*-coumaric acid derivatives. *FEBS Lett.* 374:157–160.

Karplus, M. 2000. Aspects of protein reaction dynamics: deviations from simple behavior. *J. Phys. Chem. B.* 104:11–27.

Karstens, T., and K. Kobe. 1980. Rhodamine B and rhodamine 101 as reference substances for fluorescence quantum yield measurements. *J. Phys. Chem.* 84:1871–1872.

Koeberg, M., M. de Groot, J. W. Verhoeven, N. R. Lokan, M. J. Shephard, and M. N. Paddon-Row. 2001. U-shaped donor [bridge] acceptor systems with remarkable charge transfer fluorescent properties: an experimental and computational investigation. *J. Phys. Chem. A.* 105: 3417–3424.

Kort, R., W. D. Hoff, M. Van West, A. R. Kroon, S. M. Hoffer, K. H. Vlieg, W. Crielaand, J. J. Van Beeumen, and K. J. Hellingwerf. 1996. The xanthopsins: a new family of eubacterial blue-light photoreceptors. *EMBO J.* 15:3209–3218.

Lee, B. C., P. A. Croonquist, T. R. Sosnick, and W. D. Hoff. 2001. Pas domain receptor photoactive yellow protein is converted to a molten globule state upon activation. *J. Biol. Chem.* 276:20821–20823.

Meyer, T. E., M. A. Cusanovich, and G. Tollin. 1993. Transient proton uptake and release is associated with the photocycle of the photoactive yellow protein from the purple phototrophic bacterium *Ectothiorhodospira halophila*. *Arch. Biochem. Biophys.* 306:515–517.

Meyer, T. E., G. Tollin, J. H. Hazzard, and M. A. Cusanovich. 1989. Photoactive yellow protein from the purple phototrophic bacterium, *Ectothiorhodospira halophila*: quantum yield of photobleaching and effects of temperature, alcohols, glycerol, and sucrose on kinetics of photobleaching and recovery. *Biophys. J.* 56:559–564.

Meyer, T. E., E. Yakali, M. A. Cusanovich, and G. Tollin. 1987. Properties of a water-soluble, yellow protein isolated from a halophilic phototrophic bacterium that has photochemical activity analogous to sensory rhodopsin. *Biochemistry.* 26:418–423.

Perman, B., V. Srajer, Z. Ren, T. Teng, C. Pradervand, T. Ursby, D. Bourgeois, F. Schotte, M. Wulff, R. Kort, K. Hellingwerf, and K. Moffat. 1998. Energy transduction on the nanosecond time scale: early structural events in a xanthopsin photocycle. *Science.* 279:1946–1950.

Rubinstenn, G., G. W. Vuister, F. A. Mulder, P. E. Dux, R. Boelens, K. J. Hellingwerf, and R. Kaptein. 1998. Structural and dynamic changes of photoactive yellow protein during its photocycle in solution [see comments]. *Nat. Struct. Biol.* 5:568–570.

Sackett, D. L., and J. Wolff. 1987. Nile red as a polarity-sensitive fluorescent probe of hydrophobic protein surfaces. *Anal. Biochem.* 167: 228–234.

Salamon, Z., T. E. Meyer, and G. Tollin. 1995. Photobleaching of the photoactive yellow protein from *Ectothiorhodospira halophila* promotes binding to lipid bilayers: evidence from surface plasmon resonance spectroscopy. *Biophys. J.* 68:648–654.

Sarkar, N., K. Das, D. N. Nath, and K. Bhattacharyya. 1994. Twisted charge-transfer process of nile red in homogeneous solution and in faujasite zeolite. *Langmuir.* 10:326–329.

Takeshita, K., N. Hirota, Y. Imamoto, M. Kataoka, F. Tokunaga, and M. Terazima. 2000. Temperature-dependent volume change of the initial step of the photoreaction of photoactive yellow protein (PYP) studied by transient grating. *J. Am. Chem. Soc.* 122:8524–8528.

van Brederode, M. E., T. Gensch, W. D. Hoff, K. J. Hellingwerf, and S. E. Braslavsky. 1995. Photoinduced volume change and energy storage associated with the early transformations of the photoactive yellow protein from *Ectothiorhodospira halophila*. *Biophys. J.* 68:1101–1109.

Van Brederode, M. E., W. D. Hoff, I. H. Van Stokkum, M. L. Groot, and K. J. Hellingwerf. 1996. Protein folding thermodynamics applied to the photocycle of the photoactive yellow protein. *Biophys. J.* 71:365–380.

van der Horst, M. A., I. H. van Stokkum, W. Crielaard, and K. J. Hellingwerf. 2001. The role of the N-terminal domain of photoactive yellow protein in the transient partial unfolding during signalling state formation. *FEBS Lett.* 497:26–30.

Xie, A., W. D. Hoff, A. R. Kroon, and K. J. Hellingwerf. 1996. Glu46 donates a proton to the 4-hydroxycinnamate anion chromophore during the photocycle of photoactive yellow protein. *Biochemistry.* 35: 14671–14678.

Xie, A., L. Kelemen, J. Hendriks, B. J. White, K. J. Hellingwerf, and W. D. Hoff. 2001. Formation of a new buried charge drives a large-amplitude protein quake in photoreceptor activation. *Biochemistry.* 40:1510–1517.